


 Cite this: *RSC Adv.*, 2026, 16, 19657

# Thermodynamic insights on desalination processes: exergy analysis, minimum separation work, and advances in capacitive deionization with battery electrodes

 Ayoub Taktour, Abderrahman Mellalou, \* Abdelkader Outzourhit and Fouad Ghamouss \*

Desalination plays a crucial role in addressing freshwater scarcity resulting from the rising population, industrial expansion, and the impacts of climate change. It employs various technologies tailored to varying levels of salinity. While energy efficiency is a primary focus in desalination, its intuitive interpretation is challenging due to process variations. This viewpoint offers a thermodynamics-based understanding of energy consumption by examining it in terms of irreversible dissipation and minimal separation energy. This study examines the relationship between exergy variations across different desalination technologies, which provides insight into the minimum separation energy and serves as a basis for classifying desalination processes. Simultaneously, particular emphasis is placed on capacitive deionization (CDI) as an emerging desalination technology that requires only incremental advancements to overcome current limitations associated with high feed-water salinity and the restricted desalination capacity of conventional carbon-based electrodes. The integration of advanced battery materials, including sodium-ion and chloride-ion battery systems, with CDI represents a promising strategy to enhance deionization efficiency, thereby enabling the development of higher-performance desalination technologies.

 Received 24th January 2026  
 Accepted 26th March 2026

DOI: 10.1039/d6ra00658b

[rsc.li/rsc-advances](http://rsc.li/rsc-advances)

## 1 Introduction

One of the major technological, social, and economic issues of the twenty-first century is the lack of access to clean water at a reasonable price. The United Nations has declared access to clean water to be a fundamental human right.<sup>1</sup> Yet it is still unavailable to one out of seven people worldwide.<sup>2</sup> Nevertheless, it is crucial to emphasize that a significant quantity of water is primarily employed in agriculture, as well as in the extraction of oil and gas, and the manufacturing of chemicals. If the present rate of water consumption persists, a larger number of shortages are anticipated for the global population, posing a threat to ecosystems.<sup>3</sup> On a global scale, the vast majority, approximately 98%, of Earth's water is composed of seawater and brackish water.<sup>4</sup> However, only a small fraction 2.5%, of the total water supply on the planet is freshwater. Furthermore, a significant proportion of this fresh water is stored in the shape of glacial ice or deep groundwater.<sup>5</sup> Even if well distributed and abundant, seawater and brackish water cannot be directly

utilized for domestic purposes because of their high salt concentration. For that reason, desalination as shown in Table 1, acts as an efficient and low-cost approach to reduce salt concentration and has been utilized to tackle the shortage of freshwater in areas grappling with water scarcity, including Africa, the Asia-Pacific, and the Middle East.<sup>6,7</sup>

The process of desalination of seawater or brackish water represents a viable means of obtaining freshwater for human use Fig. 1. Over the past few decades, various desalination technologies, encompassing multistage-flash distillation (MSF),<sup>16,17</sup> reverse osmosis (RO),<sup>18</sup> and electro dialysis (ED)<sup>19</sup> and Capacitive deionization (CDI).<sup>20</sup> MSF and MED necessitate elevated operating temperatures of 88–130 °C and 71 °C,<sup>8</sup> respectively, the phase transition of water from liquid to vapor, making them inherently energy-intensive processes.<sup>21</sup> On the other hand, the RO method, which utilizes high pressure to propel sea water through the RO membrane for freshwater production, requires lower energy consumption than the distillation-based techniques. Consequently, RO technology constitutes more than 60% of desalination plants worldwide.<sup>22</sup> Nevertheless, RO process faces a challenge of considerable energy consumption, predominantly attributable to the substantial pressure needed (2800 kPa for seawater and 140 kPa for brackish water<sup>9</sup>). Additionally, the RO membrane is

College of Chemical Sciences and Engineering (CCSE), Department of Materials Science, Energy and Nano-engineering (MSN), Mohammed VI Polytechnic University (UM6P), 43150 Benguerir, Morocco. E-mail: Fouad.ghamouss@um6p.ma; Abderrahman.mellalou@um6p.ma



susceptible to fouling and to mechanical damage.<sup>23,24</sup> In contrast, interfacial solar steam generation (ISSG) is a solar-driven desalination technology that localizes photothermal conversion at the air water interface, minimizing bulk water heating and reducing thermal losses.<sup>25,26</sup> ISSG materials include carbon-based structures, plasmonic nanostructures, and self-floating membranes, achieving solar-to-vapor conversion efficiencies exceeding 80%.<sup>27,28</sup> Biomass-derived materials, such as functionalized wood sponges, possess hierarchical porosity, low thermal conductivity, and capillary-driven water transport, supporting efficient interfacial evaporation.<sup>29</sup> Wood sponges coated with graphene flake/polyaniline nanocomposites provide high light absorption, enhanced photothermal conversion, and salt resistance.<sup>30</sup> These material properties enable high evaporation rates, stable operation under high salinity, and reduced thermal losses. ISSG systems are scalable, energy-efficient, and represent an alternative to conventional thermal and membrane-based desalination, technologies.<sup>26,29</sup> It's worth noticing that all the technologies are essentially focused on separating water from salt. Conversely, fresh water can be generated through electrodialysis by electrically propelling ions across ion exchange membranes, with a typical operating voltage range of approximately 2–3 V.<sup>19,31</sup> However, this voltage surpasses the theoretical threshold for water splitting. This not only diminishes charge efficiency due to side redox reactions but also results in significant electrode corrosion.<sup>32,33</sup> Additionally, energy consumption rises with increasing salt content in the feed, making the process nearly impractical when

salt concentration exceeds  $3 \text{ g}^{-1}$ , a value significantly lower than the salinity of seawater.<sup>34,35</sup>

Capacitive deionization (CDI) has surfaced as an alternative approach to water desalination,<sup>36–38</sup> offering potential benefits such as energy efficiency, environmental friendliness, and effective salt removal.<sup>31–33</sup> A standard CDI cell comprises a set of electrodes with opposite charges, resembling a supercapacitor operating at room temperature and standard pressure. During a typical CDI operation, as saline water passes through the two porous electrodes subjected to a voltage below 2 V,<sup>31</sup> ions are electrically attracted to electrodes with opposite charges in a process known as electrostatic adsorption, leading to the removal of salt ions from the solution. Unlike reverse osmosis (RO), which depends on high pressure to transport a significant fraction of water across the membrane, the CDI process directly eliminates salt ions from the incoming water.<sup>39</sup>

Technological maturity of desalination methods was quantified using a normalized bibliometric maturity index (MI) based on cumulative citations:

$$MI = (N_i - N_{\min}) / (N_{\max} - N_{\min}) \quad (1)$$

where  $N_i$  is the total citation count for technology (i), and  $N_{\min}$  and  $N_{\max}$  represent the minimum and maximum citation values across the evaluated technologies. This normalized indicator provides an objective proxy for technological development intensity and is conceptually aligned with bibliometric growth analysis,<sup>40</sup> innovation diffusion theory,<sup>41</sup> and established technology readiness assessment frameworks. Based on cumulative



**Ayoub Taktour**

*Ayoub Taktour received his master's degree in materials science and engineering, specializing in materials for energy storage, from Mohammed VI Polytechnic University in 2022. He is currently pursuing a PhD focused on desalination via capacitive deionization driven by faradaic reactions. His research interests center on Aqueous Rechargeable Batteries (ARB), Capacitive Deionization (CDI), Desalination Batteries (DB), and electrochemistry.*



**Abderrahman Mellalou**

*Mellalou Abderrahman holds a PhD degree in Renewable Energies–Energetics–Biomass and Waste Valorization–Environment from Cadi Ayyad University, Faculty of Sciences Semlalia. He is currently a Scientist at the Mohammed VI Polytechnic University (UM6P), within the MSN Department. His research focuses on hydrogen production from waste and biomass through advanced thermochemical conversion pathways. Dr MELLALOU is actively working on the development of advanced processes for hydrogen ( $H_2$ ) production and carbon valorization, aiming to enhance efficiency, sustainability, and the generation of high value-added products. His work integrates innovative thermochemical and physicochemical approaches to optimize resource recovery from biomass and waste streams. His expertise includes biomass conversion technologies, advanced thermochemical processes, laser and plasmolysis technologies for value-added product production, carbon materials development, and the integration of sustainable energy systems with a particular emphasis on green hydrogen production and carbon valorization.*



Table 1 Feed water, cost, and energy consumption of different desalination technologies<sup>8–15</sup>

Desalination technologies	Feed water	Energy consumption (kWh m <sup>-3</sup> )	Cost (US \$ per m <sup>3</sup> )	Ref.
Capacitive deionization (CDI)	Brackish water	0.05–0.59	0.11	10 and 11
Electrodialysis (ED)	Brackish water	1.6–2.3	0.47	9
Reverse osmosis (RO)	Brackish water	0.7–2	0.39–1.5	9
	Seawater	1.6–12	0.55–1	12
Multi-stage flash distillation (MSF)	Brackish water	12.7–15	7.56	8 and 13
	Seawater	25–200	0.8–1.5	14 and 15

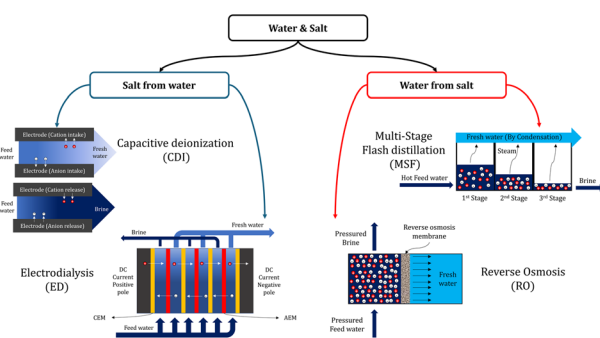


Fig. 1 Schematic diagram for desalination technologies.

citation metrics, reverse osmosis (MI = 1.00) and distillation (MI = 0.77) are classified as mature technologies, whereas capacitive deionization (MI = 0.23) is considered developing, and electrodialysis (MI ≈ 0.00) demonstrates comparatively low bibliometric maturity, indicating an earlier stage of technological consolidation relative to reverse osmosis and distillation systems. The quantity of citations in the capacitive deionization field has been experiencing exponential growth in recent years as depicted in Fig. 2. Researchers have delved into capacitive deionization from two fundamental viewpoints: the architectural perspective, and the materials perspective.<sup>42</sup> In the architecture of capacitive deionization, electro-sorption occurs on two electrodes containing the active material, the electrodes can be either attached to a framework (static) or positioned to flow within the channel of the system as depicted in Fig. 3. Among



Abdelkader Outzourhit

*Abdelkader Outzourhit holds a PhD degree in Applied Physics from the Colorado School of Mines, Golden, CO, USA, a master's degree in physics from the same School and a bachelor degree from the Cadi Ayyad University. He is currently a professor at the department of physics of the Faculty of Sciences, Cadi Ayyad University (in Marrakech, Morocco) and an affiliate to the MSN department of the Mohamed VI polytechnic*

*University UM6P(Benguerir). His research is centered on the fabrication of novel, efficient solar cells and the integration of renewable energy sources in novel applications including green hydrogen production and power to X. He participated in several EU-funded projects on renewable energies, desalination and hybrid systems and also led several national projects on renewables. He participated in several Erasmus+ projects such as AFREQEN, PROEMED and INNOMED destined to boosting quality, renewables and energy efficiency in Africa. He authored and co-authored more than 250 articles covering thin films, solar cells, renewable energies, bio-energy, hydrogen systems, batteries and photo-catalysis. His expertise includes the integration of renewable energy, coating techniques, novel pyrolysis and plasmolysis techniques.*



Fouad Ghamouss

*Prof. Fouad Ghamouss is a distinguished electrochemist specializing in energy storage and conversion technologies. He holds a PhD and HDR in electrochemistry from Université de Nantes, with expertise in lithium batteries, supercapacitors, and green hydrogen production. Ghamouss serves as a Full Professor at Mohammed VI Polytechnic University (UM6P) since April 2022, leading energy transition initiatives focused on*

*green hydrogen and large-scale battery storage. Previously, he was an Associate Professor at Université de Tours from 2009 to 2022, where he supervised 16 PhD students and managed projects on electrochemical storage with partners like SAFT, Solvay, and EDF.*



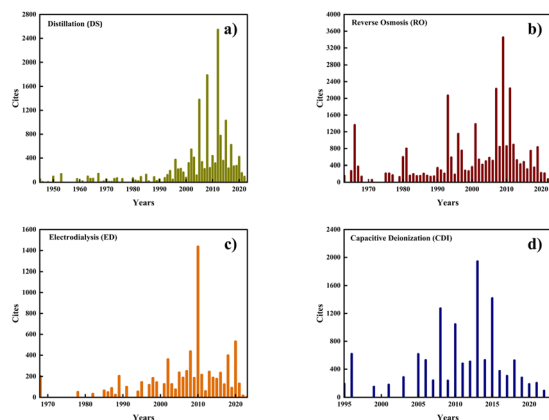


Fig. 2 Number of citations per year for (a) distillation, (b) reverse osmosis, (c) electrodialysis and (d) capacitive deionization.

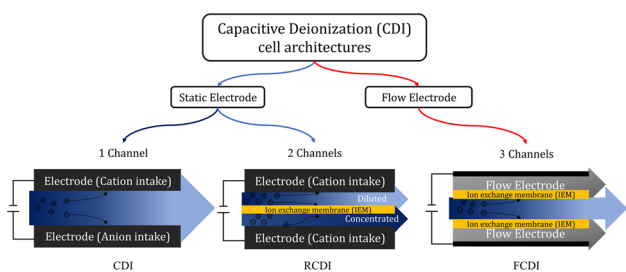


Fig. 3 Capacitive deionization (CDI) cell architectures.

different structural designs, researchers often opt for a setup featuring two porous carbon film electrodes positioned parallel to each other, leaving a narrow planar gap between them for water flow, known as the classical CDI geometry.<sup>43</sup> This configuration is also referred to as flow-by CDI. Alternatively, instead of water flowing along the electrodes, it can be directed straight through them, a method pioneered by Newman and Johnson<sup>44</sup> and further developed by Suss,<sup>45</sup> in this approach, the feed water is pumped perpendicular to the layered structure, passing through the larger pores in the electrodes. Nonetheless, these architectures demonstrate restricted electro-sorption performance due to the co-ion expulsion effect.<sup>46</sup> This phenomenon pertains to the process wherein co-ions adsorbed on the electrode surface, are released into the bulk solution when voltage is applied, leading to an increase in salinity. To

address this constraint, researchers have introduced ion exchange membranes alongside the electrodes, a configuration known as Membrane Capacitive Deionization (MCDI) (Fig. 4).<sup>47</sup> The incorporation of the membrane effectively eliminates the co-ion expulsion effect, leading to improved electro-sorption performance. Consequently, different structures have been developed to improve electro-sorption efficiency. Lee *et al.*<sup>48</sup> introduced a Hybrid Capacitive Deionization (HCDI) that integrates two separate materials, one capacitive and one faradaic. The combined effect of the two materials significantly improves electro-sorption performance, through reversible faradaic reactions, the faradaic material extracts cations from the salt solution, while the carbon electrode takes up anions.<sup>49</sup> Additionally, there have been reports of rocking-chair desalination (RCDI), a process that incorporates ion-specific pre-intercalation material as an electrode.<sup>50</sup> The mechanism, which is similar to that of intercalation batteries, *e.g.* Li-ion, Na-ion, entails the intercalation of ions within one electrode and simultaneous de-intercalation from the opposite electrode. Meanwhile, ions with an opposite charge are compelled through an ion-exchange membrane into their respective channels.<sup>51</sup> Inverted capacitive deionization (i-CDI) is a significant subset of CDI that typically employs carbon materials with fixed negative and positive charges. During cell discharge, ions are adsorbed, and the opposite process occurs during charging.<sup>52</sup> Unlike traditional CDI, (i-CDI) reverses this process by desalinating without the need for a charging operation and instead achieves recovery during charging.<sup>53</sup> For instance, a cell utilizing (i-CDI) with  $\text{MnO}_2$  and polypyrrole-coated activated carbon ( $\text{MnO}_2/\text{PPy}@AC$ ) exhibits distinct salt removal abilities.<sup>54</sup>

From materials standpoint, a multitude of highly efficient materials have been explored thus far. Initially, carbon-based materials were widely selected for capacitive deionization experiments due to their high specific surface area and relatively low cost. The electro-sorption performance of carbon-based materials is regulated by electrical double layers (EDLs). However, the effectiveness of electro-sorption in carbon-based materials is constrained by electrical double layers and co-ion expulsion.<sup>55</sup> The constraints associated with carbon-based materials have been addressed by incorporating faradaic materials with redox-active surfaces<sup>56</sup> and ion insertion materials.<sup>57</sup>

## 2 Overview of exergy variation in desalination technologies

### 2.1 Energy and exergy concepts in desalination systems

Exergy and energy are distinct concepts crucial for analyzing thermal systems. While energy adheres to the conservation principle of the first law of thermodynamics,<sup>58</sup> exergy represents usable energy for work.<sup>59</sup> Exergy provides a standardized basis for comparing interactions and assessing system efficiency by quantifying energy dissipation,<sup>60,61</sup> linked to entropy generation by the second law of thermodynamics.<sup>60</sup> Exergy is divided into physical (mechanical and thermo-mechanical) and chemical

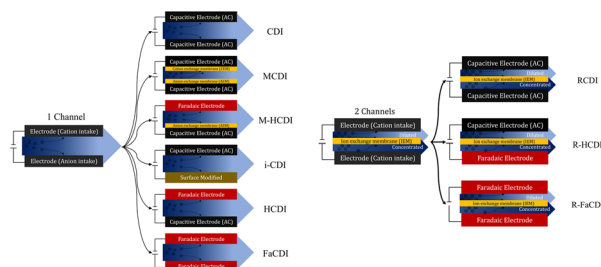


Fig. 4 Different types of capacitive deionization (CDI) categorized based on the number of channels.



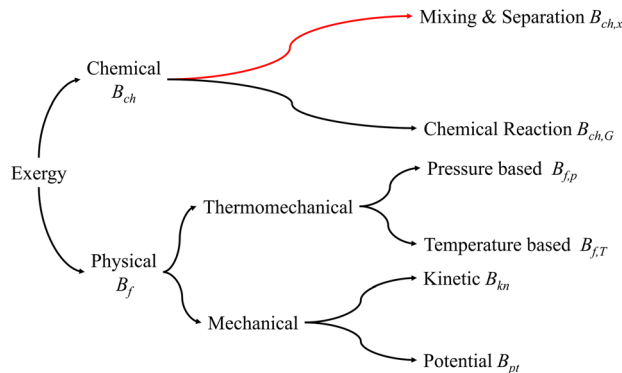


Fig. 5 Classification of exergy.

categories Fig. 5. While thermal desalination methods consider all exergy forms, membrane-based processes often overlook heat-related exergy. Notably, electrodialysis and capacitive deionization rely on chemical and electrical exergy.<sup>62</sup> Overall, desalination processes utilize various forms of exergy.<sup>63</sup> For instance, distillation processes involve high temperatures and phase changes, causing notable exergy losses due to irreversibilities like heat transfer and pressure drops. RO systems suffer from exergy losses due to pressure drops, membrane fouling, and concentration polarization. CDI systems face exergy losses from electrical resistance, electrode degradation, and inefficiencies in ion adsorption/desorption processes.

## 2.2 Exergy analysis, dead state, and thermodynamic behaviour

Exergy analysis is used to optimize energy conversion systems and to reduce losses. The main objective for all desalination processes is to convert sea water into fresh water with an external energy source. Therefore, exergy measures the potential work that can be harnessed from a resource in comparison to an environmental benchmark, facilitating a comprehensive comparison with other desalination methods.<sup>64</sup> The environment, more appropriately as exergy reference, is called the dead state Fig. 6. A dead state is any reservoir big enough so that its variables do not undergo any changes during the analyzed process, or during the interaction with the system. As often in thermodynamic analysis, different environments can be defined for different systems (*e.g.*, a river in a coal power plant,

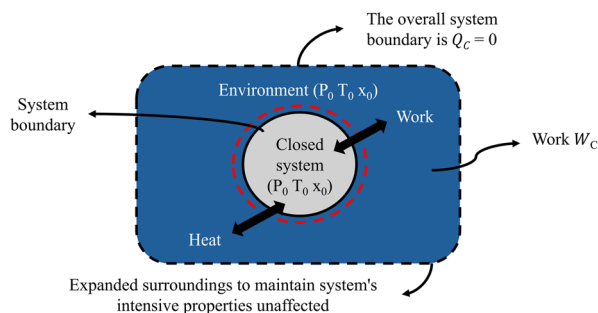


Fig. 6 Schematic illustration of a closed system in equilibrium with the environment.

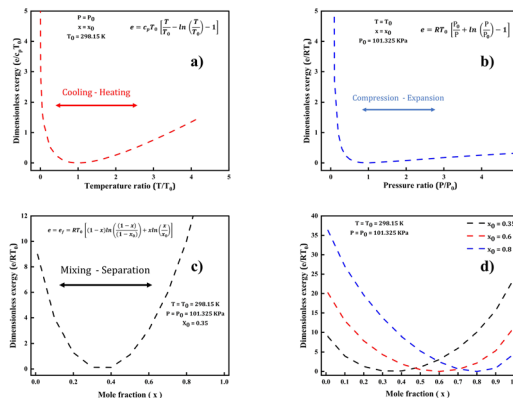


Fig. 7 Dimensionless exergy as a function of (a) temperature ratio, (b) pressure ratio, (c) mole fraction and different mole fraction.

or the outside air in a heat pump or solar thermal system). We can represent the exergy, denoted as  $e$  through mathematical expression.<sup>65,66</sup> M. H. Sharqawy *et al.*<sup>67</sup> investigated how the exergy of a control mass system evolves regarding the initial state's temperature, pressure, and mass concentration in comparison to the environment's dead state at  $T_0 = 25\text{ }^\circ\text{C}$ ,  $P_0 = 101.325\text{ kPa}$ ,  $x_0 = 0.035$  which corresponds to standard state of sea water. Under conditions ( $P_0 = P$ ;  $x_0 = x$ ;  $T_0 \neq T$ ) Fig. 7(a), exergy remains positive regardless of temperature which results in positive exergy due to potential heat transfer. When ( $T_0 = T$ ;  $x_0 = x$ ;  $P_0 \neq P$ ) Fig. 7(b), exergy stays positive at any pressure, as it allows mechanical work *via* expansion ( $P > P_0$ ) or compression ( $P < P_0$ ) to reach the environmental pressure. Additionally, when ( $T_0 = T$ ;  $P_0 = P$ ;  $x_0 \neq x$ ) Fig. 7(c), at ( $x = x_0$ ), exergy drop to zero. The second derivative consistently stays positive, confirming that ( $x = x_0$ ) is a minimum. Exergy remains positive and only nears zero when concentration matches  $x_0 = 0.035$ , as it offers work potential from mass transfer processes. In summary, the exergy of the control mass system consistently remains positive under varying temperature, pressure, and mass concentration conditions, as discussed above.

## 2.3 Technology analogies, reference state shifts, and separation metrics

In the three scenarios mentioned, each variable bears a resemblance to various desalination technology, such as thermal-driven, pressure-driven, and electrochemical-driven approaches. Additionally, as exergy assesses the potential work relative to a reference Fig. 8, we can observe two distinct states in each case where the derivative of the exergy is either negative or positive. From a desalination perspective, the state (2) resembles different analogies. For temperature, it aligns with Distillation, for pressure, it corresponds to reverse osmosis (RO), and mass concentration parallels Capacitive Deionization (CDI). In contrast, the state (1) resembles for temperature similarities to Freeze Crystallization,<sup>68</sup> while for pressure, it parallels Forward Osmosis,<sup>69</sup> and for mass concentration, it mirrors capacitive mixing CAPMIX.<sup>70</sup> Capacitive mixing aims to harness energy from differences in salinity, such as those between sea and river waters. CAPMIX relies on the voltage



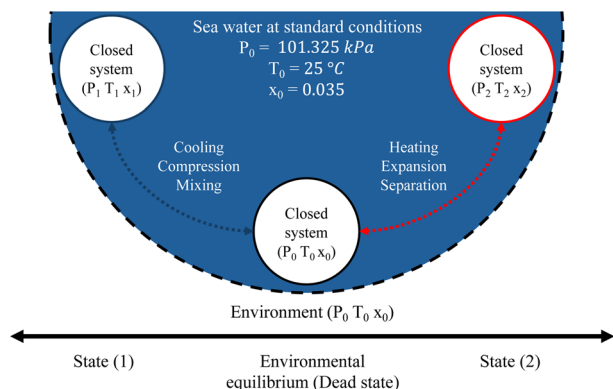


Fig. 8 Example of exergy variation of sea water.

increase occurring between two electrodes submerged in a saline solution when its salt concentration changes Fig. 9. Notably, we can observe similarities between these technologies based on whether they operate thermodynamically in a clockwise or counterclockwise fashion. For instance, in the case of ( $T_0 = T$ ;  $P_0 = P$ ;  $x_0 \neq x$ ) and by modifying the dead state Fig. 7(c), we can observe a shift in the curve and alterations in exergy over each reference state. Additionally, we can identify that the pivotal element in each process where, for instance, in CAPMIX, the critical feed is fresh water, whereas in CDI, it is the saline water feed.

Moreover, exergy analysis has been conducted on different desalination methods,<sup>71</sup> and the calculated theoretical exergy destruction values for thermal desalination, reverse osmosis, and membrane capacitive deionization (MCDI) vary, with figures of approximately 320, 64, and 8 J mol<sup>-1</sup>, respectively.<sup>63,72</sup> However, it is worth noting that chemical exergy appears to show similarity with another energy function often used for physical and chemical equilibrium in Chemical Engineering Thermodynamics called Gibbs free energy, which represents the alteration in free energy that occurs as molecules undergo a change in state, whether through mixing, transport, or chemical reactions.<sup>73</sup> Consequently, as our primary focus is on the separation process, specifically desalination by capacitive deionization, it is important to briefly examine the Gibbs energy

of separation. This will provide a foundational understanding to compare the major desalination methods.

### 3 Separation and mixing in desalination

#### 3.1 Gibbs free energy of separation and thermodynamic limits

The Gibbs free energy of separation represents the minimal energy needed to split a mixture into its individual components, without considering the specific method used.<sup>74</sup> Therefore, when it comes to desalination, it is theoretically unfeasible to extract salt from water with an amount of energy lower than the Gibbs free energy of separation. This value is equal in magnitude to the Gibbs free energy of mixing and is calculated as the difference between the Gibbs free energy of the fully mixed solution and the sum of the Gibbs free energy of each component in the mixture.<sup>75</sup> Nevertheless, the fundamental thermodynamic rule stating that any separation necessitates a minimum specific energy consumption, remains valid even when dealing with non-ideal solutions.<sup>76</sup> Li Wang *et al.*<sup>77</sup> determined the Gibbs free energy of separation for saline water and utilized this information to establish the minimum specific energy consumption ( $SEC_{min}$ ) for desalination which is essentially the Gibbs free energy of separation divided by the volume of produced water. The expression for the Gibbs free energy of mixing in an ideal two-component solution containing a generic salt species (s) and water (w) is as follows.

$$\Delta_{mix}G = nRT[x_s \ln(x_s) + x_w \ln(x_w)] \quad (2)$$

$n$  (in moles) represents the total moles of the solution containing both species,  $R$  (in J mol<sup>-1</sup> K<sup>-1</sup>) is the ideal gas constant,  $T$  (in K) is the absolute temperature and  $x$  is the mole fraction of each component in the mixture. Furthermore, by assuming a highly diluted salt solution and making use of a Taylor series expansion, particularly when ( $x_s$ ) is significantly less than 1, the Gibbs free energy of mixing becomes:

$$\Delta_{mix}G = nRT[x_s \ln(x_s) + (1 - x_s) \ln(1 - x_s)] \approx nRTx_s[\ln(x_s) - 1] \quad (3)$$

As depicted in Fig. 10(a), the Gibbs free energy of separation in a desalination process, denoted as  $\Delta_{sep}G$ , is the difference

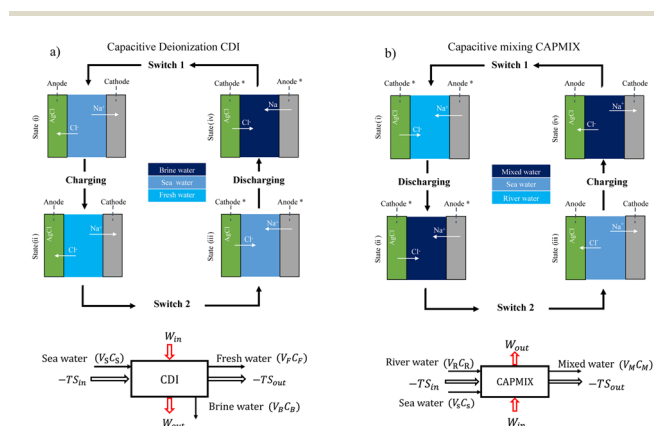


Fig. 9 Schematic representation of (a) capacitive deionization CDI and (b) capacitive mixing CAPMIX.

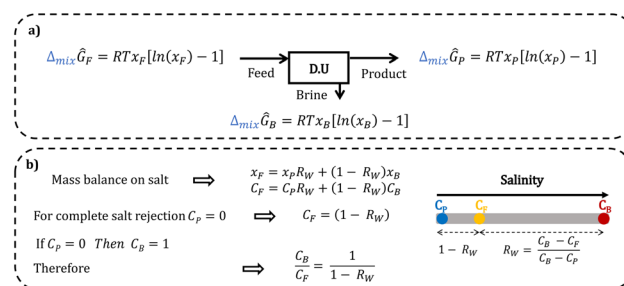


Fig. 10 (a) The primary streams of a desalination unit, (b) mass balance on salt for desalination process.



between the free energy of mixing for the produced streams of product (P) and Brine (B) water, and the free energy of mixing for the initial feedwater (F):

$$\Delta_{\text{sep}}G = \Delta_{\text{mix}}G_{\text{P}} + \Delta_{\text{mix}}G_{\text{B}} - \Delta_{\text{mix}}G_{\text{F}} \quad (4)$$

A general separation process can be characterized by several factors, including the concentration of the initial feed ( $C_{\text{F}}$ ), the concentration of the resulting product water ( $C_{\text{P}}$ ), the concentration of the brine ( $C_{\text{B}}$ ), and water recovery ( $R_{\text{w}}$ ), which is the ratio of permeate and the feed water flow rates. Three of these parameters are considered independent according to the salt mass balance. Visually, any separation can be represented using a straightforward separation line depicted in Fig. 10(b) which contains all the necessary information to define a separation. What's interesting and practical is that we can directly determine the water recovery ( $R_{\text{w}}$ ) from this line. The minimum specific energy consumption ( $\text{SEC}_{\text{min}}$  in  $\text{Wh m}^{-3}$ ) in desalination is the Gibbs free energy of separation per unit volume of product water, and is given by:

$$\text{SEC}_{\text{min}} = \frac{\Delta_{\text{sep}}\hat{G}}{R_{\text{w}}\hat{V}_{\text{w}}} = \frac{R_{\text{w}}\Delta_{\text{mix}}\hat{G}_{\text{P}} + (1 - R_{\text{w}})\Delta_{\text{mix}}\hat{G}_{\text{B}} - \Delta_{\text{mix}}\hat{G}_{\text{F}}}{R_{\text{w}}\hat{V}_{\text{w}}} \quad (5)$$

where  $\Delta_{\text{sep}}\hat{G}$  is the molar free energy of separation for given stream, and  $\hat{V}_{\text{w}}$  is the molar volume of water. Replacing  $\Delta_{\text{mix}}\hat{G}_{\text{P}}$ ,  $\Delta_{\text{mix}}\hat{G}_{\text{F}}$ , and  $\Delta_{\text{mix}}\hat{G}_{\text{B}}$  by their expressions and considering the salt mass balance, and using concentration instead of mole fractions, and assuming complete salt rejection, the specific energy consumption (SEC) is simplified to:<sup>75,78</sup>

$$\text{SEC}_{\text{min}} = -\frac{\pi_{\text{f}}}{R_{\text{w}}} \ln(1 - R_{\text{w}}) \quad (6)$$

where  $\pi_{\text{f}}$  is feed-water osmotic pressure is given by the van't Hoff relation ( $\pi_{\text{f}} = 2RTC_{\text{f}}$ ),<sup>79</sup> the Thermodynamic Energy Efficiency (TEE) is defined as the ratio between  $\Delta_{\text{sep}}G$  and  $\text{SEC}_{\text{min}}$  a desalination process:

$$\text{TTE} = \frac{\Delta_{\text{sep}}G}{\text{SEC}_{\text{min}}} \quad (7)$$

Considering a desalination process where total salt rejection is attained, the minimum thermodynamic energy consumption is determined exclusively by two factors which are the osmotic pressure ( $\pi_{\text{f}}$ ) of the feed stream and the water recovery ratio ( $R_{\text{w}}$ ).<sup>75</sup>

### 3.2 Energy consumption and efficiency across desalination technologies

Thermodynamic energy efficiency (TEE) is the fundamental quantity for evaluating desalination technologies which has been applied for methodical performance assessments. Długołęcki and van der Wal *et al.*<sup>80</sup> employed this concept, and it was subsequently revisited systematically by Hemmatifar *et al.*<sup>81</sup> Moreover, Li Wang *et al.* have more recently incorporated this concept.<sup>76</sup> In this study, we will adopt a similar approach. Although attempts have been made to incorporate

a wide range of representative data, it's important to note that this summary is only intended to cover capacitive deionization (CDI). To illustrate, let's take an example of desalinating seawater, which typically contains  $35 \text{ g L}^{-1}$  corresponding to an osmotic pressure of 29.7 bar, and assume a 50% water recovery rate. In this situation, independently of the desalination method employed, the specific energy consumption is at least  $1.1 \text{ kWh m}^{-3}$  of clean water.<sup>70,73,75</sup> Shihong Lin *et al.*<sup>78</sup> and Li Wang *et al.*<sup>76</sup> have compiled comprehensive data not only on desalination technologies but also specifically on capacitive deionization. In this study, we aim to merge both datasets, focusing more precisely on the distinct types of capacitive deionization from a materials perspective. When contrasting this data (see SI) with the reference dashed line representing the thermodynamic reversible processes ( $\text{SEC} = \Delta G_{\text{w}}$ ) in Fig. 11(a) and (b), it becomes evident that thermal desalination methods are known for their elevated energy consumption, typically between  $[1.0\text{--}1.8 \text{ kWh m}^{-3}]$ .<sup>82,83</sup> On the other hand, in the literature, it is evident that (ED) and (RO) systems have demonstrated higher energy consumption, with values of the specific Gibbs free energy of the feed water ( $\Delta G_{\text{w}}$ ) ranging from approximately  $[0.02\text{--}0.48 \text{ kWh m}^{-3}]$  for (ED)<sup>84,85</sup> and around  $[0.02\text{--}1.45 \text{ kWh m}^{-3}]$  for (RO).<sup>86,87</sup> However, (CDI) exhibits a comparatively modest ( $\Delta G_{\text{w}}$ ) due to the partial desalination of low-salinity feedwater. Most documented (CDI) processes show ( $\Delta G_{\text{w}}$ ) values in the range of  $[10^{-4}\text{--}10^{-2} \text{ kWh m}^{-3}]$ .<sup>88,89</sup> However, when intercalation materials are used as electrodes for seawater desalination, the ( $\Delta G_{\text{w}}$ ) can reach approximately  $[10^{-1} \text{ kWh m}^{-3}]$ .<sup>90</sup>

Reverse Osmosis (RO), is recognized as the cutting-edge desalination technology and has been employed for treating feed water across a broad spectrum of salinity levels, encompassing seawater, brackish water, and treated wastewater.<sup>91</sup> Although a recent study conducted a theoretical analysis comparing (RO) and (CDI),<sup>92</sup> there is a notable absence of adequate experimental data in the literature to estimate the energy consumption of (RO) when used for treating extremely low-salinity feedwater, a task typically undertaken by (CDI). In general, the summarized data indicates a positive correlation

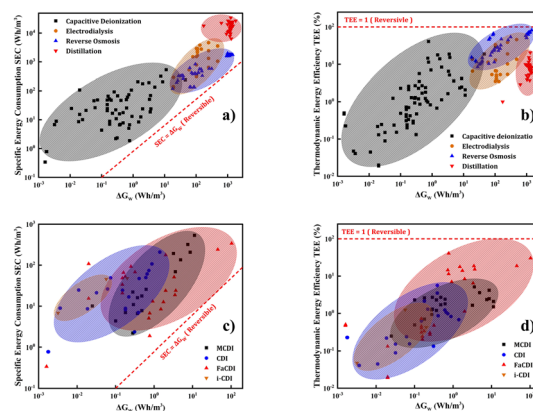


Fig. 11 (a) SEC vs.  $\Delta G_{\text{w}}$ , and (b) TEE vs.  $\Delta G_{\text{w}}$ , for the major desalination technologies, (c) SEC vs.  $\Delta G_{\text{w}}$ , and (d) TEE vs.  $\Delta G_{\text{w}}$ , for the major capacitive deionization systems.



between (SEC) and ( $\Delta G_w$ ) for both pressure-driven and electrochemical desalination processes. Notably, the data points for (RO) are situated closer to the line representing thermodynamically reversible processes, implying that (RO) generally exhibits higher energy efficiency.<sup>76,78</sup> Fig. 11(a) can be transformed into a chart displaying (TEE) *versus* ( $\Delta G_w$ ) Fig. 11(b), highlighting that (TEE) also demonstrates a positive correlation with ( $\Delta G_w$ ) for non-thermal desalination processes. In other words, achieving a higher (TEE) is generally more attainable for more challenging separations with higher energy consumption.

### 3.3 In the context of CDI using carbon electrodes

In the context of CDI using carbon electrodes, the energy consumption for desalination is commonly one to three orders of magnitude greater than the energy consumption required for achieving the desired separation. The highest levels of (TEE) appear to be predominantly attained through the utilization of CDI involving intercalation materials. Generally, when CDI processes are operated to accomplish a separation that is considered more challenging due to a greater ( $\Delta G_w$ ), they tend to exhibit higher (TEE). Fig. 11(d), reveals that while the absolute energy consumption, as measured by Specific Energy Consumption (SEC), is generally quite modest for most Capacitive Deionization CDI processes, the energy efficiency of CDI in terms of (TEE) is relatively low. This is primarily due to the typically minimal differences in Gibbs free energy associated with the separations accomplished through CDI. Most CDI processes that utilize carbon electrodes have efficiencies (TEE) that do not exceed 10%. However, in recent CDI studies employing intercalation materials as electrodes, (TEE) values exceeding 10% were attained, with the highest achieving 40%.<sup>93</sup> This level of efficiency falls within the same range as Reverse Osmosis (RO), which represents state-of-the-art desalination technology.

The summary of (TEE) based on experimental studies does not provide an understanding of why certain desalination processes are more efficient than others, nor does it inform on potential strategies for improving (TEE). To bridge this gap and offer a more intuitive understanding of (TEE), simplified analyses of energy efficiency for specific desalination methods have been done by Lin *et al.*<sup>91</sup> These analyses are meant to provide a straightforward interpretation of (TEE) without the need for detailed and rigorous process modelling. Thermal distillation is inherently demanding in terms of energy consumption because it involves phase changes. To attain a superior (TEE) in thermal distillation processes, they need to be applied to desalinate feedwater with elevated salinity and effectively recover a substantial amount of latent heat. This higher (TEE) is particularly anticipated when desalinating extremely salty brine. As a result of inherent limitations in energy efficiency, thermal distillation technologies have seen a decline in the seawater desalination market over the past few decades.<sup>94</sup> The reversible nature of RO operation means that only a small portion of energy is used to create the driving force. This interpretation remains valid unless the feed water's salinity is exceptionally low. In cases where the feed salinity is so minimal

that it becomes insignificant compared to the minimum pressure needed to overcome membrane resistance and hydraulic resistance within the module, the (TEE) of RO may decrease significantly.

This straightforward understanding of (TEE) provides insights into enhancing the energy efficiency of CDI. Enhancing (TEE) is achievable when the energy stored in Electric Double Layers (EDLs) is entirely recuperated.<sup>80,95</sup> It's important to highlight that neither the energy used during the charging process, nor the energy stored in the EDLs can be completely regained. The theoretically recoverable energy corresponds to the energy consumed during charging, minus the energy losses due to resistance in both the charging and discharging phases. The pursuit of intercalation materials as promising CDI electrode material has been primarily driven by the belief that they can yield much higher specific capacity as compared to conventional carbon-based electrodes.<sup>96,97</sup> The increased capacity is a result of intercalation materials capability to retain ions within their solid phase, specifically within the crystal structure,<sup>98,99</sup> in contrast to carbon electrodes, which store ions by creating Electric Double Layers (EDLs) within micropores. Certain Capacitive Deionization (CDI) processes employing intercalation material-based electrodes achieved notably superior TEE compared to CDI using carbon electrodes. In fact, TEE values exceeding 10% were exclusively attained in the context of intercalation-based CDI. Consequently, it is evident that electrochemical-driven methods are advantageous in scenarios with low concentrations of feed water, as opposed to pressure-driven methods, which prove favorable in high concentrations Fig. 12(a). Nevertheless, by increasing water recovery in electrochemical-driven, a discernible shift in electrochemically driven approaches toward the theoretical limit can be observed, as illustrated in Fig. 12(b). Hence, conventional capacitive deionization (CDI) performs optimally with low to moderate salinity feeds because ion removal occurs through electro-sorption in electrical double layers within porous carbon electrodes,<sup>100</sup> a mechanism that intrinsically limits salt uptake capacity and charge efficiency at high ionic strength.<sup>101</sup> With increasing salinity, shorter Debye length, enhanced co-ion repulsion, and more pronounced parasitic faradaic reactions reduce effective charge storage and raise the specific energy demand per unit of removed salt.<sup>102</sup> Moreover, highly conductive electrolytes intensify leakage currents and electrode polarization losses,<sup>103</sup> while the restricted pore volume of carbon electrodes bound total ion storage.<sup>45</sup> As a result, CDI becomes

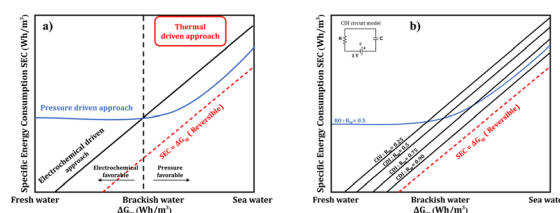


Fig. 12 (a) Conceptual diagram of energy consumption *versus* feedwater salinity for different desalination approaches and (b) energy estimates for RO and CDI *versus* feedwater concentration.



energetically and operationally unfavorable for high-salinity streams compared with pressure-driven or thermal desalination technologies. Consequently, conventional CDI is generally confined to brackish and mildly saline waters,<sup>104</sup> whereas treatment of higher salinity feeds typically relies on modified configurations such as membrane CDI or intercalation-based electrode systems.<sup>105</sup> Consequently, the pivotal factor in capacitive deionization lies in the choice of the active material.

## 4 Electrode materials for capacitive deionization

From an electrochemical perspective, capacitive deionization is the process of storing energy in the electrodes, and the subsequent regeneration of the electrodes is the delivery of the energy.<sup>106</sup> CDI process could be closely related to the behavior of the batteries and supercapacitors.<sup>107</sup> Batteries typically possess greater capacities compared to supercapacitors, primarily due to the redox reactions taking place in the battery electrode materials, which facilitate a more extensive charge transfer process.<sup>108</sup> The boundaries between battery materials and pseudocapacitive materials aren't clearly defined, as both are rooted in redox reactions.<sup>109</sup> In recent years, there has been rapid development in rechargeable battery materials,<sup>110</sup> with diverse materials featuring remarkable electrochemical properties emerging in the literature. Some of these materials have already found applications in industrial production, a promising future for integrating capacitive deionization (CDI) technology with battery materials.<sup>111</sup> Battery materials typically possess a substantial theoretical specific capacity, and this could potentially enhance the desalination capability of the CDI systems.<sup>112</sup> Nevertheless, it is important to consider certain factors when choosing electrode materials for CDI systems based on batteries. The electrode is submerged in water during the desalination process, necessitating a material that remains undissolved and water-attracting (hydrophilic) to ensure complete interaction between the ions and the material. Additionally, it's crucial for any redox reactions to take place within the water's voltage range to prevent water decomposition. Moreover, the ions in the water can become hydrated, resulting in larger sizes, which imposes a stricter demand on the structure of battery materials, to prevent deterioration during the charging and discharging procedures.<sup>111</sup> Considerable attention has been directed toward developing carbon materials featuring greater specific surface areas, enhanced electrical conductivity, and extended durability in their usage cycles. Nanoporous carbons and intercalation electrodes, while both exhibiting high selectivity, rely on distinct mechanisms, each with their relative advantages and disadvantages in selectively removing crucial species from feed waters. Notably, commercial activated carbons, a type of nanoporous carbon, can be cost-effective.<sup>113</sup> Therefore, classical Capacitive Deionization (CDI) systems may continue to be highly appealing, particularly when considering desalination performance metrics normalized by electrode cost.

In summary as depicted in Fig. 13, the electrode materials for Capacitive Deionization (CDI) include Electric Double Layer

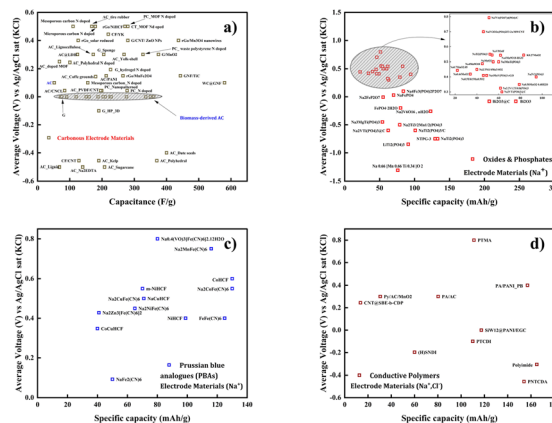


Fig. 13 Average voltage (V) vs. specific capacity ( $\text{mAh g}^{-1}$ ) for (a) carbonous materials, (b) oxides and phosphates materials, (c) Prussian blue analogues materials and (d) conductive polymers.

(EDL) capacitive materials and pseudo-capacitor ion storage materials. Notably, the desalination efficiency experienced a significant improvement when a carbon aerogel electrode was introduced in CDI,<sup>114</sup> replacing the conventional porous carbon. Furthermore, mesoporous carbon provides not just a substantial specific surface area but also effective adsorption sites.<sup>115</sup> The presence of excessively small micropores can result in the double layer overlap effect, which hinders ion desorption and is thus unfavorable.<sup>116</sup> Yet, carbon with hierarchical porosity, featuring two or more distinct pore structures concurrently, facilitates rapid migration in macropores comparable to the diffusion rate in the solution. This is attributed to the ion buffer layer formed in the macropore, which minimizes the distance from the solution to the inner surface.<sup>117</sup> CNT electrodes display a mesoporous reticular structure that is advantageous for electrosorption.<sup>118</sup> On the other hand, graphene possesses a distinctive interlayer structure that facilitates swift ion transfer.<sup>119</sup> In practical applications, graphene is frequently combined with other adsorption materials to impede graphene aggregation and enhance its adsorption capability. The synergistic effects result in graphene-based composite electrodes exhibiting superior performance in capacitance values, conductive behavior, cyclic stability, and rate performance.<sup>119</sup> Therefore, in the pursuit of enhancing performance, the combination of intercalation materials with carbon-based substances has yielded promising outcomes due to the synergistic impact of the pseudocapacitive properties of intercalation materials and the formation of the electric double layer (EDL) in carbon-based materials.<sup>120</sup> However, despite the impressive desalination capabilities reported, the majority of systems utilizing intercalation materials face constraints in effectively eliminating anions, such as chloride ions. Consequently, ion exchange membranes are frequently employed, leading to elevated costs in capacitive deionization (CDI) systems.<sup>121</sup> Despite the difficulty associated with eliminating anions, these systems demonstrate a preference for cations. For example, sodium manganese oxides (NMO) have been identified as having a specific affinity for removing  $\text{Na}^+$  ions,<sup>122,123</sup> while



NiHCF exhibits selectivity for  $K^+$  ions.<sup>124</sup> A similar pattern was observed by Kim *et al.*,<sup>57</sup> when they employed NMO to segregate  $Na^+$  from a solution containing multiple ions ( $Na^+$ ,  $K^+$ ,  $Ca^{2+}$  and  $Mg^{2+}$ ). This selectivity offers substantial promise for the application of intercalation materials across diverse domains where the precise elimination of particular ions is required, including areas like resource reclamation, water conditioning, fluoride reduction, and the extraction of heavy metals.

Desalination with battery materials<sup>125</sup> involves the removal of sodium and chloride ions from a solution, making it evident that aqueous sodium-ion and aqueous chloride-ion battery materials should hold significant roles in CDI systems. Among these, sodium-ion battery materials have garnered substantial attention and momentum in research due to their higher energy density and power density. This has led to the emergence of a diverse array of sodium-ion battery materials in CDI literature, many of which demonstrate commendable desalination performance. However, lithium-ion battery materials show greater promise for application in the desalination industry, as they are already being produced on a large scale, setting them apart from other battery materials.<sup>126</sup> MXene nanosheets tend to reassemble easily because of the robust van der Waals forces between them, which significantly impairs their ability to store electrical charge. Hence, the enhancement of MXene materials' specific capacitance could be achieved by developing effective techniques to prevent nanosheet restacking and intentionally augmenting and exploiting the space between MXene layers.<sup>127</sup> The identification of redox activity in Prussian Blue (PB) marked a pivotal moment in the evolution of intercalation electrodes. Subsequently, there was a gradual expansion in the exploration of the electrochemical properties of intercalation electrodes, with systematic efforts to comprehend and elucidate their redox-active behavior.<sup>128</sup> Notably, the study of the electrochemical characteristics of analogues of PB promptly followed the discovery of the electronic activity of pure PB.<sup>129</sup> Nevertheless, these materials were not promptly utilized for water desalination. Their application in desalination only transpired after it was established that they were suitable for sodium-ion batteries. Beyond PB, redox activity has been more recently identified in other substances such as  $MnO_2$ ,<sup>130</sup>  $Na_2FeP_2O_7$ ,<sup>131</sup> and  $NaTi_2(PO_4)_3$ ,<sup>131</sup> and these have subsequently proven successful in Capacitive Deionization (CDI).

The Na-storage electrodes utilized in desalination batteries are typically those previously employed in Na-ion and Li-ion batteries. Generally, these materials store and release  $Na^+$  through intercalation into a host structure without undergoing significant structural changes. Consequently, many Na-storage electrodes demonstrate robust cyclability when an appropriate electrolyte is chosen to enhance their performance. However, the electrolyte adjustment for desalination batteries cannot follow the same approach as Na-ion batteries. Desalination batteries are specifically designed for desalination, and as such, the electrolyte in the desalination cell must be a neutral saline solution. Therefore, it is crucial to identify Na-storage electrodes that exhibit reliable cyclability in neutral saline solutions and subsequently optimize their performance. On the other hand, research on chloride-ion battery materials is comparatively

restricted, primarily focusing on Bi-based and Ag-based materials due to chloride's limited compatibility with other substances.<sup>132</sup> A shortage of appropriate intercalation materials capable of retaining anions in water-based environments still exists. Despite Ag/AgCl serving as an exceptionally effective electrode material for Cl ion storage,<sup>133</sup> the expensive nature of silver likely constrains the widespread adoption of capacitive deionization (CDI) as a cost-effective, widely accessible technology. Prospective avenues for the storage of chloride ions in desalination systems can draw insight from the growing domain of chloride ion batteries, in which metal oxychlorides like VOCl and FeOCl have been explored as materials for cathodes.<sup>134</sup> Only two metals, namely Ag and Bi, are recognized for their ability to undergo reversible electrochemical reactions to store and release  $Cl^-$ , with their chlorinated forms remaining stable in neutral saline solutions. Unlike Na-storage electrodes, both Ag and Bi undergo phase transformations during  $Cl^-$  storage, resulting in the formation of AgCl and BiOCl, respectively. The storage and release of one  $Cl^-$  require one electron for Ag, while Bi necessitates three electrons for the same purpose. Consequently, Bi either requires three times the charge of Ag or has three times the capacity of Ag when removing  $Cl^-$ . Furthermore, up to this point, only Ag, Bi,<sup>10</sup> PPy,<sup>11</sup> and redox-PSQ poly(silsesquioxane)<sup>12</sup> have been documented as materials for chloride storage in desalination batteries, but these options exhibit distinct drawbacks that could impede their real-world utility. Specifically, Ag and PPy are expensive, Bi is hazardous, and its substantial voltage hysteresis during desalination–salination cycles, along with a low operating potential, which may result in hydrogen evolution and could result in elevated energy consumption.

Salination represents the opposite process of desalination, and the Gibbs free energy changes ( $\Delta G$ ) associated with these processes are non-zero.<sup>13</sup> When we graphically represent all the faradaic materials, as depicted in Fig. 14(b), we observe the emergence of two configurations. Consequently, one of these processes must be thermodynamically uphill (charging process,  $\Delta G > 0$ ,  $E_{cell} < 0$ ), while the other must be thermodynamically

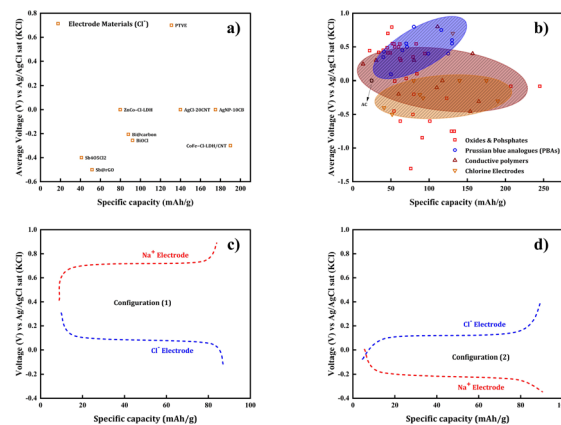


Fig. 14 Average voltage (V) vs. specific capacity ( $mAh\ g^{-1}$ ) for (a) chloride materials, (b) FaCDI electrode material and voltage (V) vs. specific capacity ( $mAh\ g^{-1}$ ) for (c) configuration 1, (d) configuration 2.



downhill (discharging process,  $\Delta G < 0$ ,  $E_{\text{cell}} > 0$ ). Here,  $E_{\text{cell}}$  refers to the thermodynamic equilibrium cell voltage, calculated as the equilibrium cathode potential minus the equilibrium anode potential. The determination of whether a process corresponds to charging or discharging is contingent upon the selection of Na-storage and Cl-storage electrodes. In desalination, the Na-storage electrode serves as the cathode, while the Cl-storage electrode acts as the anode. Consequently, if the sodiation–desodiation potential of the Na-storage electrode surpasses the chlorination–dechlorination potential of the Cl-storage electrode, the  $E_{\text{cell}}$  is positive. In this scenario, the desalination process aligns with discharging, while the salination process corresponds to charging, indicated by a negative  $E_{\text{cell}}$ . This configuration is termed a first configuration.

A desalination battery of configuration (1) produces electrical energy output during desalination and necessitates an input of electrical energy during salination Fig. 14(c). On the contrary, when the sodiation–desodiation potential of the Na-storage electrode is lower than the chlorination–dechlorination potential of the Cl-storage electrode, a configuration (2) desalination battery is created Fig. 14(d). When developing configuration (1) and configuration (2) desalination batteries, the selection of Na-storage and Cl-storage electrodes allows for the optimization or minimization of the disparity between sodiation/desodiation potential and chlorination/dechlorination potential. This choice leads to various advantages. When the electrodes are selected to maximize the potential difference, both the energy input needed for charging and the energy output generated during discharging are also maximized. While this configuration of cell requires a higher energy input for the charging process, it's essential to view this energy not as consumed but as stored. Consequently, the cell can optimize its energy storage capabilities if it can operate with high energy recovery efficiency. Conversely, when the electrodes are chosen to minimize the potential difference, both the energy input required for charging and the energy output generated during discharging are also minimized. In this scenario, the desalination battery may not function as an efficient energy storage device, but it has the advantage of operating with minimal energy input during the charging process.

For all the configurations of desalination batteries, the overall energy consumption throughout the complete desalination–salination cycle consistently equals the discrepancy between the energy input necessary for charging and the energy output generated during discharging.<sup>14</sup> Consequently, irrespective of the chosen cell type, it is imperative to optimize the electrodes to minimize the potential difference between the forward and reverse reactions Fig. 15. Additionally, for the practical application of desalination batteries, it is crucial to significantly enhance the cyclability of Na-storage and Cl-storage electrodes beyond the levels reported thus far. Furthermore, considering that the primary objective of desalination batteries is not to provide portable power but to produce desalinated water, it is vital to fabricate large-scale electrodes capable of achieving performances comparable to those observed in proof-of-concept cells. Therefore, to mitigate uncertainties and incongruities stemming

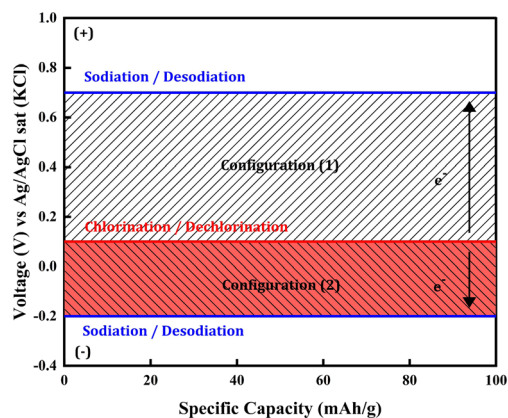


Fig. 15 Operational voltage differences between configuration 1 and 2.

from various sources and foster the advancement of desalination batteries, several recommendations are put forth by Xu D. *et al.*<sup>15</sup> The evaluation of desalination batteries necessitates the comprehensive reporting of critical performance metrics. These metrics encompass salt-removal capacity, cycle stability, energy consumption, and the Ragone plot depicts desalination capacity *versus* salt-removal rate. In scenarios where desalination processes involve both charging and discharging phases, recovering energy during the discharge process can be challenging. It is prudent to assume no energy recovery during discharge when calculating energy consumption. Standardizing electrode performance is crucial for comparability. Assessing the “half-cell” performance in a three-electrode system or a pseudo three-electrode system, utilizing a silver-based electrode as a counter/reference electrode, particularly for Na-storage materials, is recommended. Previous challenges in comparing electrode materials arise from variations in evaluating materials within the highly capacitive deionization (HCDI) system, using different types and quantities of activated carbon as a counter electrode. To enhance comparability across material systems, reporting the desalination battery's performance with a standard NaCl concentration (*e.g.*, a 1 M NaCl solution) serves as a benchmark.

The essential elements for an optimal material suitable for serving as an electrode in the field of Capacitive Deionization (CDI) encompass a substantial specific criterion, such as eco-friendly, possess a substantial salt-removal capacity (more than 100 mg per gram of active material), operate within suitable voltage ranges without triggering water electrolysis, and maintain long-term cycling stability. Additionally, it is essential to scrutinize the potential release of transition metals from these sodium-storage materials in future investigations, as it has the potential to lead to secondary pollution in the desalinated water.<sup>15,135–140</sup>

## 5 Conclusions

Desalination involves the removal of sodium and chloride ions from a solution, making sodium and chloride-ion battery materials crucial in Capacitive Deionization (CDI) systems. Lithium-ion battery materials show promise for desalination



applications due to their existing large-scale production. However, all three categories sodium-ion, chloride-ion, and lithium-ion battery materials share intercalation behavior, leading to the deterioration of crystalline structures after desalination cycles. Polymers like PPy and PANI exhibit high desalination capacities, making them ideal CDI electrode materials, while capacitive materials, such as carbon materials, offer robust cyclabilities and cost advantages. Combining the strengths of battery materials and carbon-based materials is a wise approach, yielding positive results reported by many scientists. However, it is crucial to acknowledge the profound connection between life and water, as reactions in aqueous environments are universally fundamental to life processes. This observation serves as a valuable source of inspiration for addressing the mentioned challenges. The electron shuttle in cellular metabolism relies on biomolecular redox reactions, suggesting that biomolecules with reversible redox activity hold potential for use in energy storage devices. Significantly, these redox reactions take place in tissue fluid, aligning their redox potentials precisely within the water's potential window. Compared to inorganic materials, the organic nature of biomolecules provides greater structural flexibility, facilitating the insertion and desorption of the expanded hydrated sodium or chloride ion. Additionally, the chemical diversity of biomolecules, arising from various substituent groups, renders their electrochemical properties more adaptable. Notably, the widespread presence of biomolecules in ecosystems renders them renewable and sustainable, contributing to both economic and environmental advantages in battery systems. Future research may focus on identifying environmentally friendly battery materials with large capacities in aqueous environments, incorporating them with carbonaceous materials to achieve longer cycle lives.

## Author contributions

Ayoub Taktour methodology, formal analysis, investigation, writing – original draft, writing – review & editing. Abderrahman Mellalou formal analysis, investigation, writing – review & editing, supervision. Abdelkader Outzourhit methodology, investigation, writing – review & editing. Fouad Ghamouss methodology, validation, writing – review & editing, supervision, project administration.

## Conflicts of interest

There are no conflicts to declare.

## Data availability

Data will be made available on request.

Supplementary information (SI) is available. See DOI: <https://doi.org/10.1039/d6ra00658b>.

## Acknowledgements

The authors would like to acknowledge Office Chérifien des Phosphates (OCP) and Le Ministère de l'Enseignement

Supérieur, de la Recherche Scientifique et de l'Innovation (MESRI) for financing this work.

## Notes and references

- 1 General Assembly Adopts Resolution Recognizing Access to Clean Water, Sanitation as Human Right, by Recorded Vote of 122 in Favour, None against, 41 Abstentions, 2010.
- 2 M. A. Shannon, P. W. Bohn, M. Elimelech, J. G. Georgiadis, B. J. Marias and A. M. Mayes, Science and technology for water purification in the coming decades, *Nature*, 2008, **452**, 301–310.
- 3 E. T. Sayed, M. Al Radi, A. Ahmad, M. A. Abdelkareem, H. Alawadhi, M. A. Atieh and A. G. Olabi, Faradic capacitive deionization (FCDI) for desalination and ion removal from wastewater, *Chemosphere*, 2021, **275**, 130001.
- 4 S. Manju and N. Sagar, Renewable energy integrated desalination: A sustainable solution to overcome future fresh-water scarcity in India, *Renewable Sustainable Energy Rev.*, 2017, **73**, 594–609, DOI: [10.1016/j.rser.2017.01.164](https://doi.org/10.1016/j.rser.2017.01.164).
- 5 Q. Tang and T. Oki, Terrestrial Water Cycle and Climate Change: Natural and Human-Induced Impacts, *Geophysical Monograph* 221, 2016.
- 6 M. Shatat, M. Worall and S. Riffat, Opportunities for solar water desalination worldwide: Review, *Sustain. Cities Soc.*, 2013, **9**, 67–80.
- 7 A. Al-Karaghoul and L. L. Kazmerski, Energy consumption and water production cost of conventional and renewable-energy-powered desalination processes, *Renewable Sustainable Energy Rev.*, 2013, **24**, 343–356.
- 8 S. Bhojwani, K. Topolski, R. Mukherjee, D. Sengupta and M. M. El-Halwagi, Technology review and data analysis for cost assessment of water treatment systems, *Sci. Total Environ.*, 2019, **651**, 2749–2761, DOI: [10.1016/j.scitotenv.2018.09.363](https://doi.org/10.1016/j.scitotenv.2018.09.363).
- 9 S. Burn, M. Hoang, D. Zarzo, F. Olewniak, E. Campos, B. Bolto and O. Barron, Desalination techniques — A review of the opportunities for desalination in agriculture, *Desalination*, 2015, **364**, 2–16.
- 10 J. Chang, F. Duan, C. Su, Y. Li and H. Cao, Removal of chloride ions using a bismuth electrode in capacitive deionization (CDI), *Environ. Sci.*, 2020, **6**(2), 373–382, DOI: [10.1039/c9ew00985j](https://doi.org/10.1039/c9ew00985j).
- 11 K. Xu, Y. Liu, Z. An, G. Xu, A. J. Gadgil and G. Ruan, The polymeric conformational effect on capacitive deionization performance of graphene oxide/polypyrrole composite electrode, *Desalination*, 2020, **486**, 114407, DOI: [10.1016/j.desal.2020.114407](https://doi.org/10.1016/j.desal.2020.114407).
- 12 W. Wei, *et al.*, A highly efficient porous conductive polymer electrode for seawater desalination, *J. Mater. Chem. A*, 2020, **8**(23), 11811–11817, DOI: [10.1039/d0ta03939j](https://doi.org/10.1039/d0ta03939j).
- 13 R. Zhao, *Theory and operation of capacitive deionization systems*, <https://www.researchgate.net/publication/283404850>.
- 14 D.-H. Nam, M.-A. Lumley and K.-S. Choi, Electrochemical Redox Cells Capable of Desalination and Energy Storage:



- Addressing Challenges of the Water-Energy Nexus, *ACS Energy Lett.*, 2021, **6**, 1034–1044.
- 15 D. Xu, W. Wang, M. Zhu and C. Li, Recent Advances in Desalination Battery: An Initial Review, *ACS Appl. Mater. Interfaces*, 2020, **12**, 57671–57685, DOI: [10.1021/acsami.0c15413](https://doi.org/10.1021/acsami.0c15413).
- 16 H. Baig, M. A. Antar and S. M. Zubair, Performance evaluation of a once-through multi-stage flash distillation system: Impact of brine heater fouling, *Energy Convers. Manag.*, 2011, **52**(2), 1414–1425, DOI: [10.1016/j.enconman.2010.10.004](https://doi.org/10.1016/j.enconman.2010.10.004).
- 17 K. J. Gabriel, P. Linke and M. M. El-Halwagi, Optimization of multi-effect distillation process using a linear enthalpy model, *Desalination*, 2015, **365**, 261–276, DOI: [10.1016/j.desal.2015.03.011](https://doi.org/10.1016/j.desal.2015.03.011).
- 18 L. F. Greenlee, D. F. Lawler, B. D. Freeman, B. Marrot and P. Moulin, Reverse osmosis desalination: Water sources, technology, and today's challenges, *Water Research*, 2009, **43**, 2317–2348.
- 19 H. Strathmann, Electrodialysis, a mature technology with a multitude of new applications, *Desalination*, 2010, **264**(3), 268–288, DOI: [10.1016/j.desal.2010.04.069](https://doi.org/10.1016/j.desal.2010.04.069).
- 20 T. J. Welgemoed and C. F. Schutte, Capacitive Deionization Technology™: An alternative desalination solution, *Desalination*, 2005, **183**(1–3), 327–340, DOI: [10.1016/j.desal.2005.02.054](https://doi.org/10.1016/j.desal.2005.02.054).
- 21 R. B. Saffarini, E. K. Summers, H. A. Arafat and J. H. Lienhard V, Technical evaluation of stand-alone solar powered membrane distillation systems, *Desalination*, 2012, **286**, 332–341, DOI: [10.1016/j.desal.2011.11.044](https://doi.org/10.1016/j.desal.2011.11.044).
- 22 A. Deshmukh, C. Boo, V. Karanikola, S. Lin, A. P. Straub, T. Tong, D. M. Warsinger and M. Elimelech, Membrane distillation at the water-energy nexus: limits, opportunities, and challenges, *EEnergy Environ. Sci.*, 2018, **11**, 1177–1196.
- 23 M. Wilf and C. Bartels, Optimization of seawater RO systems design, *Desalination*, 2005, **173**(1), 1–12, DOI: [10.1016/j.desal.2004.06.206](https://doi.org/10.1016/j.desal.2004.06.206).
- 24 F. J. García Latorre, S. O. Pérez Báez and A. Gómez Gotor, Energy performance of a reverse osmosis desalination plant operating with variable pressure and flow, *Desalination*, 2015, **366**, 146–153, DOI: [10.1016/j.desal.2015.02.039](https://doi.org/10.1016/j.desal.2015.02.039).
- 25 A. Ghasemi, S. Khalifi and S. Jedi, Streptozotocin-nicotinamide-induced rat model of type 2 diabetes (review), *Acta Physiol. Hung.*, 2014, **101**(4), 408–420, DOI: [10.1556/APhysiol.101.2014.4.2](https://doi.org/10.1556/APhysiol.101.2014.4.2).
- 26 S. K. Hazra, A. M. Saleque, A. K. Thakur, M. N. A. S. Ivan, D. Biswas, S. A. Khan, R. Saidur, Z. Ma and R. Sathyamurthy, Recent Advancement in Solar-Driven Interfacial Steam Generation for Desalination: A State-of-the-Art Review, *Energy Technol.*, 2024, **12**(3), DOI: [10.1002/ente.202301190](https://doi.org/10.1002/ente.202301190).
- 27 M. S. Zielinski, *et al.*, Hollow Mesoporous Plasmonic Nanoshells for Enhanced Solar Vapor Generation, *Nano Lett.*, 2016, **16**(4), 2159–2167, DOI: [10.1021/acs.nanolett.5b03901](https://doi.org/10.1021/acs.nanolett.5b03901).
- 28 G. Maqsood, *et al.*, NiMn-LDH/polypyrrole photothermal structures for interfacial solar steam generation, *Chem. Eng. J.*, 2025, **524**, 168954, DOI: [10.1016/j.cej.2025.168954](https://doi.org/10.1016/j.cej.2025.168954).
- 29 E. K. Goharshadi, *et al.*, Functionalized wood sponges: Advanced biomass materials for renewable energies, freshwater production, energy storage, and environmental remediation, *Renew. Sustain. Energy Rev.*, 2025, **209**, 115093, DOI: [10.1016/j.rser.2024.115093](https://doi.org/10.1016/j.rser.2024.115093).
- 30 M. Shafae, E. K. Goharshadi and H. Behnejad, Salt-resistant hierarchically porous wood sponge coated with graphene flake/polyaniline nanocomposite for interfacial solar steam production and wastewater treatment, *Sol. Energy*, 2024, **276**, 112707, DOI: [10.1016/j.solener.2024.112707](https://doi.org/10.1016/j.solener.2024.112707).
- 31 A. Thamilselvan, A. S. Nesaraj and M. Noel, Review on carbon-based electrode materials for application in capacitive deionization process, *Int. J. Environ. Sci. Technol.*, 2016, **13**, 2961–2976.
- 32 F. A. AlMarzooqi, A. A. Al Ghaferi, I. Saadat and N. Hilal, Application of Capacitive Deionisation in water desalination: A review, *Desalination*, 2014, **342**, 3–15.
- 33 E. García-Quismondo, C. Santos, J. Palma and M. A. Anderson, On the challenge of developing wastewater treatment processes: capacitive deionization, *Desalination Water Treat.*, 2016, **57**(5), 2315–2324, DOI: [10.1080/19443994.2014.984929](https://doi.org/10.1080/19443994.2014.984929).
- 34 D. M. Warsinger, S. Chakraborty, E. W. Tow, M. H. Plumlee, C. Bellona, S. Loutatidou, L. Karimi, A. M. Mikelonis, A. Achilli, A. Ghassemi, L. P. Padhye, S. A. Snyder, S. Curcio, C. D. Vecitis, H. A. Arafat and J. H. Lienhard, A review of polymeric membranes and processes for potable water reuse, *Prog. Polym. Sci.*, 2018, **81**, 209–237.
- 35 O. S. Burheim, F. Seland, J. G. Pharoah and S. Kjelstrup, Improved electrode systems for reverse electro-dialysis and electro-dialysis, *Desalination*, 2012, **285**, 147–152, DOI: [10.1016/j.desal.2011.09.048](https://doi.org/10.1016/j.desal.2011.09.048).
- 36 H. Yin, *et al.*, Three-dimensional graphene/metal oxide nanoparticle hybrids for high-performance capacitive deionization of saline water, *Adv. Mater.*, 2013, **25**(43), 6270–6276, DOI: [10.1002/adma.201302223](https://doi.org/10.1002/adma.201302223).
- 37 B. Han, G. Cheng, Y. Wang and X. Wang, Structure and functionality design of novel carbon and faradaic electrode materials for high-performance capacitive deionization, *Chem. Eng. J.*, 2018, **360**, 364–384.
- 38 M. A. Ahmed and S. Tewari, Capacitive deionization: Processes, materials and state of the technology, *J. Electroanal. Chem.*, 2018, **813**, 178–192.
- 39 M. Zhang and W. Kong, Recent progress in graphene-based and ion-intercalation electrode materials for capacitive deionization, *J. Electroanal. Chem.*, 2020, **878**, 114703.
- 40 J. C. Mankins, *Technology Readiness Levels*.
- 41 E. M. Rogers, *Diffusion of Innovations*, Free Press, 1995.
- 42 S. D. Datar, R. Mane and N. Jha, Recent progress in materials and architectures for capacitive deionization: A



- comprehensive review, *Water Environ. Res.*, 2022, DOI: [10.1002/wer.10696](https://doi.org/10.1002/wer.10696).
- 43 S. Porada, R. Zhao, A. Van Der Wal, V. Presser and P. M. Biesheuvel, Review on the science and technology of water desalination by capacitive deionization, *Prog. Mater. Sci.*, 2013, **58**, 1388–1442.
- 44 A. M. Johnson and J. Newman, Desalting by Means of Porous Carbon Electrodes, *J. Electrochem. Soc.*, 1971, **118**, 510.
- 45 M. E. Suss, *et al.*, Capacitive desalination with flow-through electrodes, *Energy Environ. Sci.*, 2012, **5**(11), 9511–9519, DOI: [10.1039/c2ee21498a](https://doi.org/10.1039/c2ee21498a).
- 46 P. M. Biesheuvel and A. van der Wal, Membrane capacitive deionization, *J. Membr. Sci.*, 2010, **346**(2), 256–262, DOI: [10.1016/j.memsci.2009.09.043](https://doi.org/10.1016/j.memsci.2009.09.043).
- 47 P. M. Biesheuvel and A. van der Wal, Membrane capacitive deionization, *J. Membr. Sci.*, 2010, **346**(2), 256–262, DOI: [10.1016/j.memsci.2009.09.043](https://doi.org/10.1016/j.memsci.2009.09.043).
- 48 J. Lee, S. Kim, C. Kim and J. Yoon, Hybrid capacitive deionization to enhance the desalination performance of capacitive techniques, *Energy Environ. Sci.*, 2014, **7**(11), 3683–3689, DOI: [10.1039/c4ee02378a](https://doi.org/10.1039/c4ee02378a).
- 49 C. Wang, L. Chen and L. Zhu, Effect of combined fouling on desalination performance of membrane capacitive deionization (MCDI) during long-term operation, *J. Dispers. Sci. Technol.*, 2020, **41**(3), 383–392, DOI: [10.1080/01932691.2019.1579654](https://doi.org/10.1080/01932691.2019.1579654).
- 50 J. Lee, S. Kim and J. Yoon, Rocking Chair Desalination Battery Based on Prussian Blue Electrodes, *ACS Omega*, 2017, **2**(4), 1653–1659, DOI: [10.1021/acsomega.6b00526](https://doi.org/10.1021/acsomega.6b00526).
- 51 K. C. Smith and R. Dmello, Na-Ion Desalination (NID) Enabled by Na-Blocking Membranes and Symmetric Na-Intercalation: Porous-Electrode Modeling, *J. Electrochem. Soc.*, 2016, **163**(3), A530–A539, DOI: [10.1149/2.0761603jes](https://doi.org/10.1149/2.0761603jes).
- 52 X. Gao, A. Omozebi, J. Landon and K. Liu, Surface charge enhanced carbon electrodes for stable and efficient capacitive deionization using inverted adsorption-desorption behavior, *Energy Environ. Sci.*, 2015, **8**(3), 897–909, DOI: [10.1039/c4ee03172e](https://doi.org/10.1039/c4ee03172e).
- 53 X. Gao, A. Omozebi, J. Landon and K. Liu, Enhanced Salt Removal in an Inverted Capacitive Deionization Cell Using Amine Modified Microporous Carbon Cathodes, *Environ. Sci. Technol.*, 2015, **49**(18), 10920–10926, DOI: [10.1021/acs.est.5b02320](https://doi.org/10.1021/acs.est.5b02320).
- 54 Y.-H. Tu, C.-F. Liu, J.-A. Wang and C.-C. Hu, Construction of an inverted-capacitive deionization system utilizing pseudocapacitive materials, *Electrochem. Commun.*, 2019, **104**, 106486, DOI: [10.1016/j.elecom.2019.106486](https://doi.org/10.1016/j.elecom.2019.106486).
- 55 J. Zhou, H. Zhou, Y. Zhang, J. Wu, H. Zhang, G. Wang and J. Li, Pseudocapacitive deionization of uranium(VI) with WO<sub>3</sub>/C electrode, *Chem. Eng. J.*, 2020, **398**, 125460, DOI: [10.1016/j.cej.2020.125460](https://doi.org/10.1016/j.cej.2020.125460).
- 56 P. Biesheuvel, M. Bazant, R. Cusick, T. Hatton, K. Hatzell, M. Hatzell, P. Liang, S. Lin, S. Porada, J. Santiago, K. Smith, M. Stadermann, X. Su, X. Sun, T. Waite, A. Wal, J. Yoon, R. Zhao, L. Zou and M. Suss, Capacitive Deionization – defining a class of desalination technologies, *arXiv*, 2017, arXiv:1709.05925, DOI: [10.48550/arXiv.1709.05925](https://doi.org/10.48550/arXiv.1709.05925).
- 57 S. Kim, H. Yoon, D. Shin, J. Lee and J. Yoon, Electrochemical selective ion separation in capacitive deionization with sodium manganese oxide, *J. Colloid Interface Sci.*, 2017, **506**, 644–648, DOI: [10.1016/j.jcis.2017.07.054](https://doi.org/10.1016/j.jcis.2017.07.054).
- 58 H. Struchtrup, The First Law of Thermodynamics, in *Thermodynamics and Energy Conversion*, Springer Berlin Heidelberg, Berlin, Heidelberg, 2014, pp. 33–53, DOI: [10.1007/978-3-662-43715-5\\_3](https://doi.org/10.1007/978-3-662-43715-5_3).
- 59 H. W. Hevert and S. C. Hevert, Second Law Analysis: An Alternative Indicator Of System Efficiency, *Energy*, 1980, **5**, 865–873.
- 60 I. Dincer and M. A. Rosen, Exergy and Energy Analyses, in *Exergy*, Elsevier, 2013, pp. 21–30, DOI: [10.1016/b978-0-08-097089-9.00002-4](https://doi.org/10.1016/b978-0-08-097089-9.00002-4).
- 61 R. D. Robinett and D. G. Wilson, *Exergy and irreversible entropy production thermodynamic concepts for control system design: Regulators*, Institute of Electrical Electronics Engineers, 2006, vol. 21, pp. 2249–2256.
- 62 V. G. Gude, Exergy evaluation of desalination processes, *ChemEngineering*, 2018, **2**(2), 1–27, DOI: [10.3390/chemengineering2020028](https://doi.org/10.3390/chemengineering2020028).
- 63 K. S. Splegler and Y. M. El-Sayed, *The Energetics of Desalination Processes*, 2001, <https://www.elsevier.com/locate/desal>.
- 64 I. Dincer, *The Role of Exergy in Energy Policy Making*, 2002.
- 65 *Energy and the Environment, Vol. 15*, Environmental Science and Technology Library, ed. A. Bejan, P. Vadász and D. G. Kröger, Springer Netherlands, Dordrecht, 1999, vol. 15, DOI: [10.1007/978-94-011-4593-0](https://doi.org/10.1007/978-94-011-4593-0).
- 66 A. Bejan, *Advanced Engineering Thermodynamics*, Wiley, 2016.
- 67 M. H. Sharqawy, J. H. Lienhard V and S. M. Zubair, On exergy calculations of seawater with applications in desalination systems, *Int. J. Therm. Sci.*, 2011, **50**(2), 187–196, DOI: [10.1016/j.ijthermalsci.2010.09.013](https://doi.org/10.1016/j.ijthermalsci.2010.09.013).
- 68 A. Najim, A review of advances in freeze desalination and future prospects, *npj Clean Water*, DOI: [10.1038/s41545-022-00158-1](https://doi.org/10.1038/s41545-022-00158-1).
- 69 N. Abounahia, I. Ibrar, T. Kazwini, A. Altaee, A. K. Samal, S. J. Zaidi and A. H. Hawari, Desalination by the forward osmosis: Advancement and challenges, *Sci. Total Environ.*, 2023, **886**, 163901, DOI: [10.1016/j.scitotenv.2023.163901](https://doi.org/10.1016/j.scitotenv.2023.163901).
- 70 R. Rica, R. Ziano, D. Salerno, F. Mantegazza, R. Van Roij and D. Brogioli, Capacitive Mixing for Harvesting the Free Energy of Solutions at Different Concentrations, *Entropy*, 2013, **15**, 1388–1407, DOI: [10.3390/e15041388](https://doi.org/10.3390/e15041388).
- 71 L. Fitzsimons and B. Eng, *A Detailed Study of Desalination Exergy Models and Their Application to a Semiconductor Ultra-pure Water Plant*, 2011.
- 72 P. A. Fritz, F. K. Zisopoulos, S. Verheggen, K. Schroën and R. M. Boom, Exergy analysis of membrane capacitive deionization (MCDI), *Desalination*, 2018, **444**, 162–168, DOI: [10.1016/j.desal.2018.01.026](https://doi.org/10.1016/j.desal.2018.01.026).



- 73 I. Dincer and C. Zamfirescu, Fundamentals of Thermodynamics, in *Advanced Power Generation Systems*, Elsevier, 2014, pp. 1–53, DOI: [10.1016/b978-0-12-383860-5.00001-8](https://doi.org/10.1016/b978-0-12-383860-5.00001-8).
- 74 *Chemical and Engineering Thermodynamics Solutions Manual*-Wiley.
- 75 L. Wang, C. Violet, R. M. Duchanois and M. Elimelech, Derivation of the Theoretical Minimum Energy of Separation of Desalination Processes, *J. Chem. Educ.*, 2020, **97**(12), 4361–4369, DOI: [10.1021/acs.jchemed.0c01194](https://doi.org/10.1021/acs.jchemed.0c01194).
- 76 L. Wang, J. E. Dykstra and S. Lin, Energy Efficiency of Capacitive Deionization, *Environ. Sci. Technol.*, 2019, **53**(7), 3366–3378, DOI: [10.1021/acs.est.8b04858](https://doi.org/10.1021/acs.est.8b04858).
- 77 L. Wang, J. E. Dykstra and S. Lin, Energy Efficiency of Capacitive Deionization, *Environ. Sci. Technol.*, 2019, **53**(7), 3366–3378, DOI: [10.1021/acs.est.8b04858](https://doi.org/10.1021/acs.est.8b04858).
- 78 S. Lin, Energy Efficiency of Desalination: Fundamental Insights from Intuitive Interpretation, *Environ. Sci. Technol.*, 2019, **54**, 76–84, DOI: [10.1021/acs.est.9b04788](https://doi.org/10.1021/acs.est.9b04788).
- 79 S. I. Sandler, *Chemical, Biochemical, and Engineering Thermodynamics*, 4th edn, 2006, John Wiley & Sons, Inc.
- 80 P. Długolecki and A. Van Der Wal, Energy recovery in membrane capacitive deionization, *Environ. Sci. Technol.*, 2013, **47**(9), 4904–4910, DOI: [10.1021/es3053202](https://doi.org/10.1021/es3053202).
- 81 A. Hemmatifar, A. Ramachandran, K. Liu, D. I. Oyarzun, M. Z. Bazant and J. G. Santiago, Thermodynamics of Ion Separation by Electrosorption, *Environ. Sci. Technol.*, 2018, **52**(17), 10196–10204, DOI: [10.1021/acs.est.8b02959](https://doi.org/10.1021/acs.est.8b02959).
- 82 D. Han, W. F. He, C. Yue and W. H. Pu, Study on desalination of zero-emission system based on mechanical vapor compression, *Appl. Energy*, 2017, **185**, 1490–1496, DOI: [10.1016/j.apenergy.2015.12.061](https://doi.org/10.1016/j.apenergy.2015.12.061).
- 83 D. Zhao, J. Xue, S. Li, H. Sun and Q. dong Zhang, Theoretical analyses of thermal and economical aspects of multi-effect distillation desalination dealing with high-salinity wastewater, *Desalination*, 2011, **273**(2–3), 292–298, DOI: [10.1016/j.desal.2011.01.048](https://doi.org/10.1016/j.desal.2011.01.048).
- 84 M. Demircioglu, N. Kabay, I. Kurucaovali, and E. Ersoz, Demineralization by electro dialysis (ED)-separation performance and cost comparison for monovalent salts, <https://www.elsevier.com/locate/desal>.
- 85 A. H. Galama, M. Saakes, H. Bruning, H. H. M. Rijnaarts and J. W. Post, Seawater predesalination with electro dialysis, *Desalination*, 2014, **342**, 61–69, DOI: [10.1016/j.desal.2013.07.012](https://doi.org/10.1016/j.desal.2013.07.012).
- 86 M. Busch and W. E. Mickols, Reducing energy consumption in seawater desalination, *Desalination*, 2004, **165**, 299–312, DOI: [10.1016/j.desal.2004.06.035](https://doi.org/10.1016/j.desal.2004.06.035).
- 87 M. Belkacem, S. Bekhti and K. Bensadok, Groundwater treatment by reverse osmosis, *Desalination*, 2007, **206**(1–3), 100–106, DOI: [10.1016/j.desal.2006.02.062](https://doi.org/10.1016/j.desal.2006.02.062).
- 88 S. Ahualli, G. R. Iglesias, M. M. Fernández, M. L. Jiménez and Á. V. Delgado, Use of Soft Electrodes in Capacitive Deionization of Solutions, *Environ. Sci. Technol.*, 2017, **51**(9), 5326–5333, DOI: [10.1021/acs.est.6b06181](https://doi.org/10.1021/acs.est.6b06181).
- 89 M. Pasta, C. D. Wessells, Y. Cui and F. La Mantia, A desalination battery, *Nano Lett.*, 2012, **12**(2), 839–843, DOI: [10.1021/nl203889e](https://doi.org/10.1021/nl203889e).
- 90 J. Lee, S. Kim and J. Yoon, Rocking Chair Desalination Battery Based on Prussian Blue Electrodes, *ACS Omega*, 2017, **2**(4), 1653–1659, DOI: [10.1021/acsomega.6b00526](https://doi.org/10.1021/acsomega.6b00526).
- 91 S. Lin, Energy Efficiency of Desalination: Fundamental Insights from Intuitive Interpretation, *Environ. Sci. Technol.*, 2019, **54**, 76–84, DOI: [10.1021/acs.est.9b04788](https://doi.org/10.1021/acs.est.9b04788).
- 92 M. Qin, *et al.*, Comparison of energy consumption in desalination by capacitive deionization and reverse osmosis, *Desalination*, 2019, **455**, 100–114, DOI: [10.1016/j.desal.2019.01.003](https://doi.org/10.1016/j.desal.2019.01.003).
- 93 S. Choi, B. Chang, S. Kim, J. Lee, J. Yoon and J. W. Choi, Battery Electrode Materials with Omnivalent Cation Storage for Fast and Charge-Efficient Ion Removal of Asymmetric Capacitive Deionization, *Adv. Funct. Mater.*, 2018, **28**, 1802665, DOI: [10.1002/adfm.201802665](https://doi.org/10.1002/adfm.201802665).
- 94 M. Elimelech and W. A. Phillip, The Future of Seawater Desalination: Energy, Technology, and the Environment, 2011, <http://science.sciencemag.org/>.
- 95 L. Han, K. G. Karthikeyan and K. B. Gregory, Energy Consumption and Recovery in Capacitive Deionization Using Nanoporous Activated Carbon Electrodes, *J. Electrochem. Soc.*, 2015, **162**(12), E282–E288, DOI: [10.1149/2.0431512jes](https://doi.org/10.1149/2.0431512jes).
- 96 M. E. Suss and V. Presser, Water Desalination with Energy Storage Electrode Materials, *Joule*, 2018, **2**, 10–15.
- 97 P. Srimuk, *et al.*, Faradaic deionization of brackish and sea water via pseudocapacitive cation and anion intercalation into few-layered molybdenum disulfide, *J. Mater. Chem. A*, 2017, **5**(30), 15640–15649, DOI: [10.1039/c7ta03120c](https://doi.org/10.1039/c7ta03120c).
- 98 K. C. Smith, Theoretical evaluation of electrochemical cell architectures using cation intercalation electrodes for desalination, *Electrochim. Acta*, 2017, **230**, 333–341, DOI: [10.1016/j.electacta.2017.02.006](https://doi.org/10.1016/j.electacta.2017.02.006).
- 99 K. Singh, H. J. M. Bouwmeester, L. C. P. M. De Smet, M. Z. Bazant and P. M. Biesheuvel, Theory of Water Desalination with Intercalation Materials, *Phys. Rev. Appl.*, 2018, **9**(6), DOI: [10.1103/PhysRevApplied.9.064036](https://doi.org/10.1103/PhysRevApplied.9.064036).
- 100 A. Hemmatifar, J. W. Palko, M. Stadermann and J. G. Santiago, Energy breakdown in capacitive deionization, *Water Res.*, 2016, **104**, 303–311, DOI: [10.1016/j.watres.2016.08.020](https://doi.org/10.1016/j.watres.2016.08.020).
- 101 P. M. Biesheuvel and M. Z. Bazant, Nonlinear dynamics of capacitive charging and desalination by porous electrodes, *Phys. Rev. E*, 2010, **81**(3), 031502, DOI: [10.1103/PhysRevE.81.031502](https://doi.org/10.1103/PhysRevE.81.031502).
- 102 S. Porada, *et al.*, Direct prediction of the desalination performance of porous carbon electrodes for capacitive deionization, *Energy Environ. Sci.*, 2013, **6**(12), 3700, DOI: [10.1039/c3ee42209g](https://doi.org/10.1039/c3ee42209g).
- 103 R. Zhao, S. Porada, P. M. Biesheuvel and A. Van der Wal, Energy consumption in membrane capacitive deionization for different water recoveries and flow rates, and comparison with reverse osmosis, *Desalination*, 2013, **330**, 35–41, DOI: [10.1016/j.desal.2013.08.017](https://doi.org/10.1016/j.desal.2013.08.017).



- 104 A. Hemmatifar, M. Stadermann and J. G. Santiago, Two-Dimensional Porous Electrode Model for Capacitive Deionization, *J. Phys. Chem. C*, 2015, **119**(44), 24681–24694, DOI: [10.1021/acs.jpcc.5b05847](https://doi.org/10.1021/acs.jpcc.5b05847).
- 105 X. Gao, A. Omosibi, J. Landon and K. Liu, Enhanced Salt Removal in an Inverted Capacitive Deionization Cell Using Amine Modified Microporous Carbon Cathodes, *Environ. Sci. Technol.*, 2015, **49**(18), 10920–10926, DOI: [10.1021/acs.est.5b02320](https://doi.org/10.1021/acs.est.5b02320).
- 106 Z. Guo, Y. Ma, X. Dong, M. Hou, Y. Wang and Y. Xia, Integrating Desalination and Energy Storage using a Saltwater-based Hybrid Sodium-ion Supercapacitor, *ChemSusChem*, 2018, **11**(11), 1741–1745, DOI: [10.1002/cssc.201800517](https://doi.org/10.1002/cssc.201800517).
- 107 M. Pasta, C. D. Wessells, Y. Cui and F. La Mantia, A desalination battery, *Nano Lett.*, 2012, **12**(2), 839–843, DOI: [10.1021/nl203889e](https://doi.org/10.1021/nl203889e).
- 108 M. Al, H. Gualous, N. Omar and J. Van, Batteries and Supercapacitors for Electric Vehicles, in *New Generation of Electric Vehicles*, InTech, 2012, DOI: [10.5772/53490](https://doi.org/10.5772/53490).
- 109 J. Wang, S. Dong, B. Ding, Y. Wang, X. Hao, H. Dou, Y. Xia and X. Zhang, Pseudocapacitive materials for electrochemical capacitors: from rational synthesis to capacitance optimization, *Natl. Sci. Rev.*, 2016, **4**, 71–90, DOI: [10.1093/nsr/nww072](https://doi.org/10.1093/nsr/nww072).
- 110 M. B. Sahana and R. Gopalan, Recent Developments in Electrode Materials for Lithium-Ion Batteries for Energy Storage Application, in *Handbook of Advanced Ceramics and Composites*, Springer International Publishing, 2019, pp. 1–37, DOI: [10.1007/978-3-319-73255-8\\_44-1](https://doi.org/10.1007/978-3-319-73255-8_44-1).
- 111 Y. Jiang, S. I. Alhassan, D. Wei and H. Wang, A review of battery materials as cdi electrodes for desalination, *Water*, 2020, **12**(11), 1–32, DOI: [10.3390/w12113030](https://doi.org/10.3390/w12113030).
- 112 D. H. Nam, M. A. Lumley and K. S. Choi, A Desalination Battery Combining Cu<sub>3</sub>Fe(CN)<sub>6</sub> as a Na-Storage Electrode and Bi as a Cl-Storage Electrode Enabling Membrane-Free Desalination, *Chem. Mater.*, 2019, **31**(4), 1460–1468, DOI: [10.1021/acs.chemmater.9b00084](https://doi.org/10.1021/acs.chemmater.9b00084).
- 113 T. T. T. Nguyen, L. T. N. Huynh, T. N. Pham, T. N. Tran, T. T. N. Ho, T. D. Nguyen, T. T. Nguyen, T. K. A. Vo, G. V. Pham, V. H. Le, T. T. Le, T. H. Nguyen, H. Thai, T. L. Le and D. L. Tran, Enhanced capacitive deionization performance of activated carbon derived from coconut shell electrodes with low content carbon nanotubes-graphene synergistic hybrid additive, *Mater. Lett.*, 2021, **292**, 129652, DOI: [10.1016/j.matlet.2021.129652](https://doi.org/10.1016/j.matlet.2021.129652).
- 114 D. K. Le, N. Q. Pham and K. A. Le, Capacitive deionization (CDI) for desalination using carbon aerogel electrodes, *Science and Technology Development Journal*, 2016, **19**, 155–164.
- 115 C. Tsouris, *et al.*, Mesoporous carbon for capacitive deionization of saline water, *Environ. Sci. Technol.*, 2011, **45**(23), 10243–10249, DOI: [10.1021/es201551e](https://doi.org/10.1021/es201551e).
- 116 P. M. Biesheuvel, R. Zhao, S. Porada and A. van der Wal, Theory of membrane capacitive deionization including the effect of the electrode pore space, *J. Colloid Interface Sci.*, 2011, **360**(1), 239–248, DOI: [10.1016/j.jcis.2011.04.049](https://doi.org/10.1016/j.jcis.2011.04.049).
- 117 H. Wang, *et al.*, Hierarchical Porous Carbon from the Synergistic ‘Pore-on-Pore’ Strategy for Efficient Capacitive Deionization, *ACS Sustain. Chem. Eng.*, 2020, **8**(2), 1129–1136, DOI: [10.1021/acssuschemeng.9b06084](https://doi.org/10.1021/acssuschemeng.9b06084).
- 118 L. Wang, *et al.*, Capacitive deionization of NaCl solutions using carbon nanotube sponge electrodes, *J. Mater. Chem.*, 2011, **21**(45), 18295–18299, DOI: [10.1039/c1jm13105b](https://doi.org/10.1039/c1jm13105b).
- 119 P. Liu, T. Yan, L. Shi, H. S. Park, X. Chen, Z. Zhao and D. Zhang, Graphene-based materials for capacitive deionization, *J. Mater. Chem. A*, 2017, **5**, 13907–13943, DOI: [10.1039/c7ta02653f](https://doi.org/10.1039/c7ta02653f).
- 120 B. A. Samejo, *et al.*, MXene-based composites for capacitive deionization – The advantages, progress, and their role in desalination – A review, *Water Resour. Ind.*, 2023, 100230, DOI: [10.1016/j.wri.2023.100230](https://doi.org/10.1016/j.wri.2023.100230).
- 121 J. Elisadiki and C. K. King’andu, Performance of ion intercalation materials in capacitive deionization/electrochemical deionization: A review, *J. Electroanal. Chem.*, 2020, **878**, 114588, DOI: [10.1016/j.jelechem.2020.114588](https://doi.org/10.1016/j.jelechem.2020.114588).
- 122 W. J. Shi, *et al.*, Low-Strain Reticular Sodium Manganese Oxide as an Ultrastable Cathode for Sodium-Ion Batteries, *ACS Appl. Mater. Interfaces*, 2020, **12**(12), 14174–14184, DOI: [10.1021/acsami.0c00788](https://doi.org/10.1021/acsami.0c00788).
- 123 S. Guo, *et al.*, A high-capacity, low-cost layered sodium manganese oxide material as cathode for sodium-ion batteries, *ChemSusChem*, 2014, **7**(8), 2115–2119, DOI: [10.1002/cssc.201402138](https://doi.org/10.1002/cssc.201402138).
- 124 T.-H. Chen, D. V. Cuong, Y. Jang, N.-Z. Khu, E. Chung and C.-H. Hou, Cation selectivity of activated carbon and nickel hexacyanoferrate electrode materials in capacitive deionization: A comparison study, *Chemosphere*, 2022, **307**, 135613, DOI: [10.1016/j.chemosphere.2022.135613](https://doi.org/10.1016/j.chemosphere.2022.135613).
- 125 M. Pasta, C. D. Wessells, Y. Cui and F. La Mantia, A desalination battery, *Nano Lett.*, 2012, **12**(2), 839–843, DOI: [10.1021/nl203889e](https://doi.org/10.1021/nl203889e).
- 126 S. Zahir, T. Elmakki, M. Gulied, Z. Ahmad, L. Al-Sulaiti, H. K. Shon, Y. Chen, H. Park, B. Batchelor and D. S. Han, A review on lithium recovery using electrochemical capturing systems, *Desalination*, 2020, **500**, 114883, DOI: [10.1016/j.desal.2020.114883](https://doi.org/10.1016/j.desal.2020.114883).
- 127 M. Zhang and W. Kong, Recent progress in graphene-based and ion-intercalation electrode materials for capacitive deionization, *J. Electroanal. Chem.*, 2020, **878**, 114703, DOI: [10.1016/j.jelechem.2020.114703](https://doi.org/10.1016/j.jelechem.2020.114703).
- 128 L. Guo, *et al.*, A Prussian blue anode for high performance electrochemical deionization promoted by the faradaic mechanism, *Nanoscale*, 2017, **9**(35), 13305–13312, DOI: [10.1039/c7nr03579a](https://doi.org/10.1039/c7nr03579a).
- 129 Y. Zhao, B. Liang, X. Wei, K. Li, C. Lv and Y. Zhao, A core-shell heterostructured CuFe@NiFe Prussian blue analogue as a novel electrode material for high-capacity and stable capacitive deionization, *J. Mater. Chem. A*, 2019, **7**(17), 10464–10474, DOI: [10.1039/c8ta12433g](https://doi.org/10.1039/c8ta12433g).
- 130 Z. Y. Leong and H. Y. Yang, A Study of MnO<sub>2</sub> with Different Crystalline Forms for Pseudocapacitive Desalination, *ACS*



- Appl. Mater. Interfaces*, 2019, **11**(14), 13176–13184, DOI: [10.1021/acsami.8b20880](https://doi.org/10.1021/acsami.8b20880).
- 131 S. Kim, J. Lee, C. Kim and J. Yoon, Na<sub>2</sub>FeP<sub>2</sub>O<sub>7</sub> as a Novel Material for Hybrid Capacitive Deionization, *Electrochim. Acta*, 2016, **203**, 265–271, DOI: [10.1016/j.electacta.2016.04.056](https://doi.org/10.1016/j.electacta.2016.04.056).
- 132 F. Chen, Z. Y. Leong and H. Y. Yang, An aqueous rechargeable chloride ion battery, *Energy Storage Mater.*, 2017, **7**, 189–194, DOI: [10.1016/j.ensm.2017.02.001](https://doi.org/10.1016/j.ensm.2017.02.001).
- 133 P. Srimuk, S. Husmann and V. Presser, Low voltage operation of a silver/silver chloride battery with high desalination capacity in seawater, *RSC Adv.*, 2019, **9**(26), 14849–14858, DOI: [10.1039/c9ra02570g](https://doi.org/10.1039/c9ra02570g).
- 134 X. Zhao, Z. Zhao-Karger, D. Wang and M. Fichtner, Metal oxychlorides as cathode materials for chloride ion batteries, *Angew. Chem., Int. Ed.*, 2013, **52**(51), 13621–13624, DOI: [10.1002/anie.201307314](https://doi.org/10.1002/anie.201307314).
- 135 T. J. Welgemoed and C. F. Schutte, Capacitive Deionization Technology™: An alternative desalination solution, *Desalination*, 2005, **183**(1–3), 327–340, DOI: [10.1016/j.desal.2005.02.054](https://doi.org/10.1016/j.desal.2005.02.054).
- 136 M. Mossad, W. Zhang and L. Zou, Using capacitive deionisation for inland brackish groundwater desalination in a remote location, *Desalination*, 2013, **308**, 154–160, DOI: [10.1016/j.desal.2012.05.021](https://doi.org/10.1016/j.desal.2012.05.021).
- 137 Solar Desalination for the 21 st Century, <https://www.nato.int/science>.
- 138 H. Bamufleh, F. Abdelhady, H. M. Baaqeel and M. M. El-Halwagi, Optimization of multi-effect distillation with brine treatment via membrane distillation and process heat integration, *Desalination*, 2017, **408**, 110–118, DOI: [10.1016/j.desal.2017.01.016](https://doi.org/10.1016/j.desal.2017.01.016).
- 139 N. Ghaffour, T. M. Missimer and G. L. Amy, Technical review and evaluation of the economics of water desalination: Current and future challenges for better water supply sustainability, *Desalination*, 2013, **309**, 197–207, DOI: [10.1016/j.desal.2012.10.015](https://doi.org/10.1016/j.desal.2012.10.015).
- 140 I. Hore-Lacy, Other nuclear energy applications: Hydrogen for transport desalination ships space research reactors for radioisotopes, in *Nuclear Energy in the 21st Century*, Elsevier, 2007, pp. 93–110.

